Combined Nanoindentation and Adhesion Force Mapping Using the Atomic Force Microscope: Investigations of a Filled Polysiloxane Coating

Peter Eaton,† Francis Fernández Estarlich,‡ Richard J. Ewen,§ Thomas G. Nevell,* James R. Smith, and John Tsibouklis

School of Pharmacy and Biomedical Sciences, University of Portsmouth, St. Michael's Building, White Swan Road, Portsmouth PO1 2DT, U.K.

Received July 12, 2001. In Final Form: April 15, 2002

Using atomic force microscopy, adhesion force and indentation mapping have been combined with measurements of topography in mapping the hardness variations on the surface of a $CaCO_3$-filled silicone coating material. The topographic image revealed a smooth surface with protruding features, matching the size of filler particles (1−3 μm). Mapped indentation and adhesion force measurements showed that these features were associated with increased surface hardness and, also, a suppressed ability to develop adhesive interactions with the probing material (silicon nitride). Furthermore, the indentation images revealed that a boundary region of increased softness surrounded each protruding particle.

Introduction

In the development of nontoxic coating materials to give protection against marine biofouling, some $CaCO_3$-filled elastomeric products based on poly(dimethylsiloxanes) (PDMS) or poly(dimethyldiphenylsiloxanes) have shown useful resistance.[1] The antifouling capabilities have been attributed to the combined properties of low surface energy[2] (22 mJ m^{-2}), low glass transition temperature[3] (T_g, −120 to −124 °C), and stability in water.[4] However, in inhibiting the settlement of barnacles, the softness of the material may be as important as its low surface energy.[5] The incorporation of calcium carbonate has been found to prolong the useful performance of some materials; particles close to the surface are covered with a thin film of elastomer.[2] A preliminary study of the surfaces of such materials has been conducted using atomic force microscopy (AFM) in the tapping mode.[4]

The AFM technique of adhesion force mapping has been applied to a wide variety of materials, to characterize their surface heterogeneity.[6−9] Consecutive measurements of the pull-off (adhesion) force, obtained across a surface, may be used to generate a high-resolution map of chemical heterogeneity; data are collected using an AFM cantilever with a very low spring constant, both to minimize indentation into the sample and to maximize the pull-off deflection.[10] The tip is brought into contact with the sample and then retracted; the pull-off force is measured as the minimum tension required to remove the tip from the sample.[11] The nature of the forces probed is often complex,[12] with many types of interaction, including van der Waals', capillary, and electrostatic forces contributing to the measured pull-off force.[11,13] The magnitude of the combined forces depends on factors including the surface energy characteristics of the tip and of the substrate;[8] in some cases it is also affected by topography.[14] The primary advantage of the adhesion mapping technique is its potential for investigating surface heterogeneity, with resolution limited mainly by the AFM tip radius.[10]

A complementary technique, but using a less flexible cantilever, has been used to collect indentation data. These are, in turn, used to determine mechanical properties,[14,15] and some mapping of indentation/stiffness parameters has been reported.[16−19] The application of the technique to the study of soft samples (e.g. silicone elastomers) may prove particularly useful, since there is likely to be less surface distortion and damage following retraction of the tip between each measurement. In the present work,

* To whom correspondence should be addressed.

† Now at: Instituto de Investigaciones Químicas (IIQ)−CSIC, c/Americo Vespucio s/n, Isla de la Cartuja, Sevilla 41092, Spain.

‡ Also at the Maritime Research Centre, Southampton Institute, East Park Terrace, Southampton SO14 0RP, U.K.

§ Faculty of Applied Sciences, University of the West of England, Frenchay Campus, Coldharbour Lane, Bristol BS16 1QY, U.K.

(1) Edwards, D. P.; Nevell, T. G.; Plunkett, B. A.; Ochiltree, B. C. *Int. Biodet. Biodeg.* **1994**, *34* (3−4), 349.

(2) Burnell, T. B.; Carpenter, J. C.; Carroll, K. M.; Cella, J. A.; Resue, J. A.; Rubinsztajn, G.; Serth-Guzzo, J.; Stein, J.; Truby, K. E.; Webb, K. K.; Schultz, M.; Swain, G. W.; Zimmerman, R. *Advances in Nontoxic Silicone Biofouling Release Coatings*; General Electric Corporation Research and Development Report No. 97CRD062; General Electric Corp.: 1997 (http://www.crd.ge.com/crd_reports/pdf/1997crd062.pdf).

(3) Aranguren, M. I.; Mora, E.; Macosko, C. W. *J. Colloid Interface Sci.* **1997**, *195*, 329.

(4) Bullock, S.; Johnston, E. E.; Willson. T.; Gatenholm, P.; Wynne, K. J. *J. Colloid Interface Sci.* **1999**, *210*, 18.

(5) Berglin, M.; Gatenholm, P. *J. Adhes. Sci. Technol.* **1999**, *13* (6), 713.

(6) Nie, H. Y.; Walzak, M. J.; Berno, B.; Mcintyre, N. S. *Langmuir* **1999**, *15*, 6484.

(7) Jogikalmath, G.; Stuart, J. K.; Pungor, A.; Hlady, V. *Colloids Surf. A: Physicochem. Eng.* **1999**, *154*, 53.

(8) Kawai, A.; Nagata, H.; Takata, M. *Jpn. J. Appl. Phys. Part 2−Lett.* **1992**, *31* (7B), L977.

(9) Suzuki, H.; Mashiko, S. *Thin Solid Films* **1998**, *331* (1−2), 176.

(10) Eaton, P.; Graham P.; Smith, J. R.; Smart, J. D.; Nevell, T. G.; Tsibouklis, J. *Langmuir* **2000**, *16*, 7887.

(11) Burnham, N. A.; Colton, H. M.; Pollock, H. M. *Nature* **1993**, *4*, 64.

(12) Weisenhorn, A. L.; Maivald, P.; Butt, H. J.; Hansma, P. K. *Phys. Rev. B−Condens Matter* **1992**, *45* (19), 11226.

(13) Cappella, B.; Dietler, T. *Surf. Sci. Rep.* **1999**, *34*, 1.

(14) Mizes, H. A.; Loh, K. G.; Miller, R. J. D.; Ahuja, S. K.; Grabowski, E. F. *Appl. Phys. Lett.* **1991**, *59* (22), 2901.

(15) Serre, C.; Gorostiza, P.; Perez-Rodriguez, A.; Sanz, F.; Morante, J. R. *Sens. Actuators, A* **1998**, *67* (1−3), 215.

(16) Bowen, W. R.; Lovitt, R. W.; Wright, C. J. *Biotechnol. Lett.* **2000**, *22* (11), 893.

(17) Raghavan, D.; Gu, X.; Nguyen, T.; Vanlandingham, M.; Karim, A. *Macromolecules* **2000**, *33*, 2573.

(18) Considine, R. F.; Dixon, D. R.; Drummond, C. J. *Langmuir* **2000**, *16*, 1323.

(19) Dufrêne, Y. F.; Barger, W. R.; Green, J. B. D.; Lee, G. U. *Langmuir* **1997**, *13*, 4779.

10.1021/la0110747 CCC: $22.00
Published on Web 11/09/2002

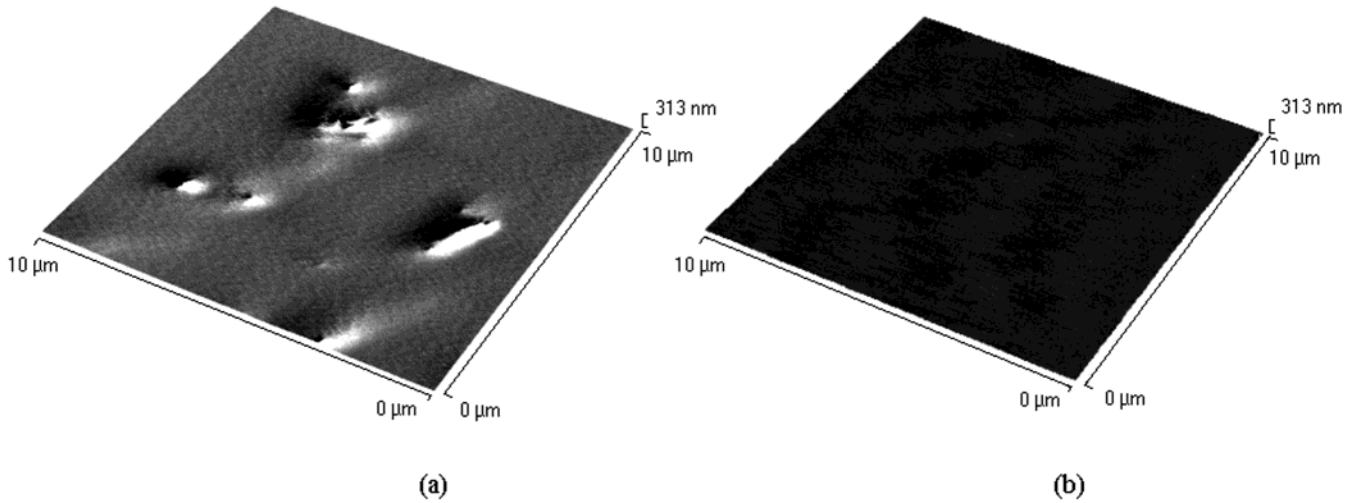

Figure 1. Topographic AFM scans of the surface of silicone elastomer GE-RTV11: (a) formulated as received (right-hand shaded) and (b) formulated after removal of filler (un-shaded).

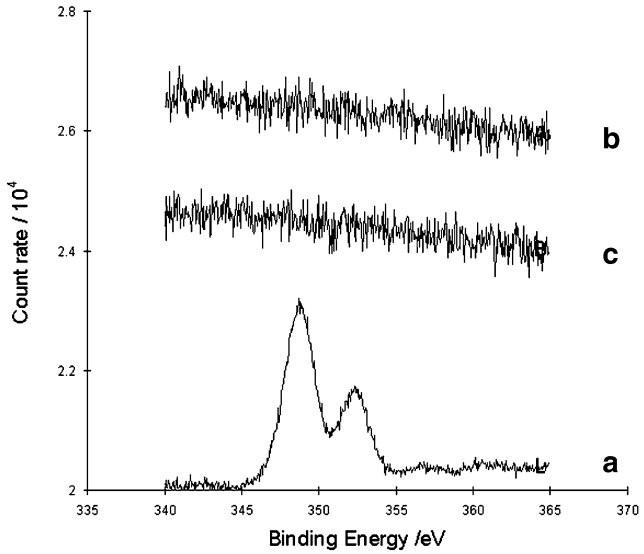

Figure 2. XPS spectrum (calcium region; Ca2p3/2 at 348 eV and Ca2p1/2 at 351 eV) for (a) a sample of pure $CaCO_3$, (b) $CaCO_3$-containing silicone elastomer GE-RTV11, and (c) silicone elastomer GE-RTV11 with the $CaCO_3$ filler removed.

topographic imaging, adhesion, and indentation mapping have been combined to examine the surface of a polymeric silicone, with particular reference to the effects of calcium carbonate filler particles on the hardness characteristics of the surface.

Experimental Section

Materials. The silicone coating material General Electric RTV11[20,21] (Techsil Ltd, Stratford-upon-Avon, U.K.) was used both as supplied (PDMS, 60−80% (w/w); $CaCO_3$, 10−30% (w/w); ethyl silicate ES40 cross-linking agent, 1.6% (w/w)) and, for the purposes of comparison, with the filler removed by centrifuging (25.5 g portions, 40 000 rpm, 2 h, to give a clear liquid—supernatant PDMS/ES40—over $CaCO_3$, 28.5% (w/w) after washing (hexane) and drying). To prepare silicone formulations, polymer/ES40 mixtures (with and without filler) were stirred (5 min) prior to the addition of dibutyltindilaurate (DBTDL, 0.1% (w/w)), the cross-linking catalyst. After further stirring (10 min) and degassing under vacuum (10 min), the freshly prepared formulations were applied by brushing (coverage 0.076 ± 0.003 g cm^{-2}) onto substrates of poly(methyl methacrylate) (10 × 10 × 2 mm, cleaned and primed with SS 4155, Techsil Ltd.) and allowed to cure (dust free; room-temperature for 48 h and then 40 °C for 2 weeks). The typical coating thickness (micrometer, five measurements per sample) was 0.86 ± 0.08 mm. Using the method of Berglin et al.,[5] the proportion of extractable un-cross-linked material in RTV11 coatings was found to be 2.7 ± 0.8%.

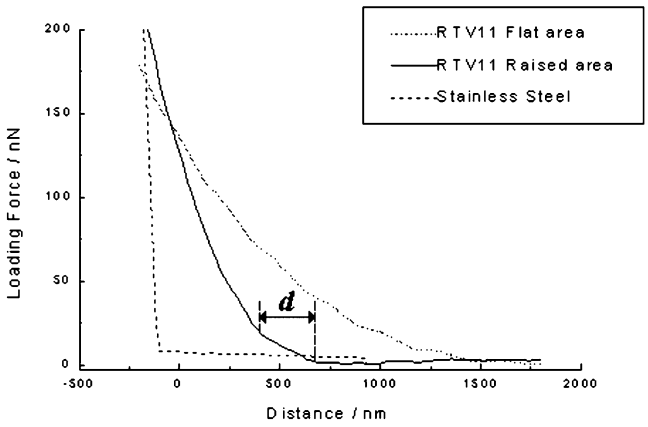

Figure 3. Resistance to indentation (deflection current) against normal displacement, for a silicon tip on a stiff cantilever (K = 37 N m^{-1}) over (a) GE-RTV11 flat area (···), (b) GE-RTV11 raised surface feature (—); and, (c) stainless steel (--). Region d corresponds with polymer film over a particle.

Stainless steel AISI 304 (Righton Ltd., Portsmouth U.K.) was used as a hard reference material.

Instrumentation. AFM was performed in air under ambient conditions using a TopoMetrix TMX2000 scanning probe microscope (ThermoMicroscopes, Bicester, U.K.) with a 70 × 70 × 12 μm tripod piezoelectric scanner. Topography and adhesion measurements were made using "V"-shaped silicon nitride cantilevers bearing an integrated standard profile tip (length, 100 μm; nominal spring constant (K), 0.21 N m^{-1}; Part. No. 1530-00, ThermoMicroscopes, Santa Clara CA).[22] The spring constant was determined, using an adaptation of Cleveland's method,[23] by measuring natural resonant frequency (ν) of the cantilever (mass m^*) after the attachment (UV-cure adhesive) of small-end masses (M) consisting of one or more monodisperse polystyrene microspheres (diameter, 40.25 ± 0.32 μm; mass, 35.9 ng; Duke Scientific Corp., Palo Alto, CA).[22] Following eq 1

$$M = K(2\pi\nu)^{-2} - m^* \qquad (1)$$

(20) Griffith, J. R. U.S. Patent 5449553, 1995.
(21) Griffith, J. R. U.S. Patent 5593732, 1997.

(22) Tsibouklis, J.; Graham, P.; Peters, V.; Eaton, P.; Smith, J. R.; Nevell, T. G.; Smart, J. D.; Ewen, R. J. *Macromolecules* **2000**, *33*, 8460.

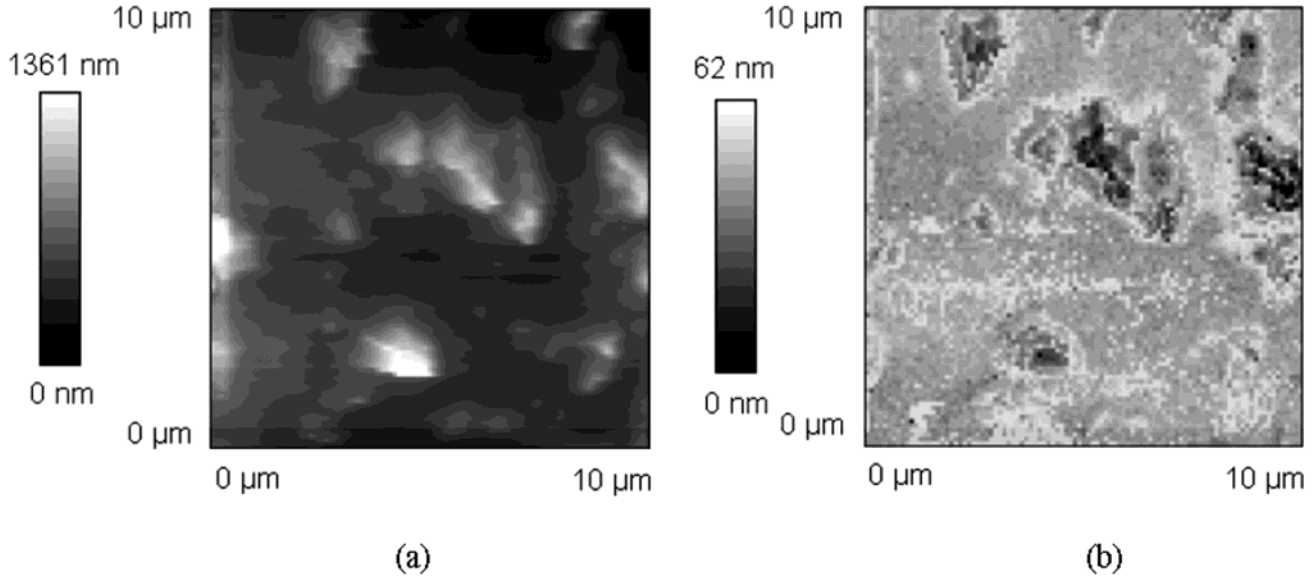

Figure 4. Indentation mapping of a selected area of the surface of GE-RTV11, using a stiff cantilever ($K = 37$ N m^{-1}) with a silicon tip: (a) topographic image (maximum deflection (light area), 1360 nm); (b) indentation under applied force of 178 nN (maximum deflection (dark area), 62 nm).

a plot of M *versus* $1/(2\pi\nu)^2$ was linear (slope $K = 0.24 \pm 0.01$ N m^{-1}); for indentation measurements, a beam-shaped silicon cantilever (Nanosensors, LOT Oriel Ltd., Leatherhead, U.K.; length, 225 μm; from dimensions and resonant frequency, $K = 37 \pm 1$ N m^{-1}) was used.

*AFM Force Measurements and Mapping.*Adhesion between the Si_3N_4 tip and polymer surfaces, in air under ambient conditions (these experiments were not performed under water since slow absorption of water gives rise to progressive changes in surface characteristics[24]) was measured by recording the deflection of the flexible cantilever at the stage at which, during the retraction regime of the force−distance curve, the tip became detached from the surface. This "pull-off" deflection (current, nA) was converted to a force of adhesion (nN) using the sensor response obtained from each force curve and the measured spring constant of the cantilever. Indentation was measured using the stiff cantilever, by recording the deflection of the cantilever during the approach cycle of the force curve, as the tip was pressed into the surface. The cantilever deflection measured against stainless steel, a hard surface relative to the material of the tip, was also recorded in the same manner.

Adhesion and indentation mapping were both achieved using the layered imaging mode of the microscope. An adhesion map was generated as gray scale image from a 50 × 50 x,y-data set of forces curves, each comprising 200 points. These maps were deconvolved from sample topography, as described elsewhere.[10] Indentation maps were produced in a similar manner from 100 × 100 force curves, each consisting of 100 points. For these maps, the brightness level at each pixel position was calculated from the nanoindentation for a given applied force over the entire data set (100 × 100 pixels), the latter usually corresponding to a scan range of 10 μm × 10 μm. For purposes of comparison the force maps, showing either adhesion or indentation, were plotted alongside the simultaneously obtained topographic image. Calculation and spatial mapping of adhesion and indentation forces were performed with programs custom-written in Microsoft Visual Basic.

Scanning Electron Microscopy. Scanning electron microscopy (SEM, with energy-dispersive X-ray analysis EDX) was performed using a JEOL 5200 instrument; samples were coated with gold (ca. 20 nm).

X-ray Photoelectron Spectroscopy. X-ray photoelectron spectroscopy (XPS) was carried out using a VG Scientific ESCALAB Mk.II employing a non-monochromatized AlKα source (1486.6 eV) operating at a power of 250 W. In all cases, the takeoff angle between electron exit and the sample surface was kept constant at 75°. The analyzer was operated at a constant pass energy of 20 eV. Line shape analysis was performed on each peak, and atomic percentages were calculated from the peak areas using standard atomic sensitivity factors;[25] the lower detection limit for O, C, Si, and Ca was 0.02 at. %.

Results

Surface Topography and Elemental Analysis. Topographic AFM images of both filled and unfilled RTV11 films are shown in Figure 1. The overall roughness (R_a) over areas of 10 μm^2 of the filled elastomer was 8.5 (std dev, 5.9) nm although both the unfilled elastomer (10 μm^2) and areas of the filled elastomer between particles (10 μm^2) were extremely smooth: R_a 0.15 (std dev, 0.02) nm and R_a 0.17 (std dev, 0.02) nm, respectively. The surfaces of filled RTV11 films contained protruding features of 1−3 μm in diameter and 0.1−0.3 μm in height; there were no protrusions from the surfaces of unfilled elastomeric films. Using SEM-EDX, calcium was detected both in the surface of the filled elastomer and in the separated filler but not in the unfilled elastomer. The mean diameter of the extracted filler particles was determined as 2.5 (std dev, 0.9) μm. For films of filled elastomer, the number of protrusions per 1000 μm^2 was determined from topographic AFM scans as 56 (std dev, 30) and from SEM as 50 (std dev, 7). Using XPS, no signal for Ca was observed for the surfaces of either of the polymer films (Figure 2). Furthermore, there were no detectable differences between the respective signals obtained for C, O, or Si. These observations correspond closely with previous work[4] and are consistent with filler particles protruding from the surface being covered with a film of elastomer, which was thicker than the depth of penetration of the probing technique (i.e. >50 nm).

Indentation Mapping with Topography. For filled elastomers, indentation measurements from flat regions of the surface and from protruding areas revealed differences in surface hardness. The force curve for the feature (Figure 3: force vs indentation distance, measured

(23) Cleveland, J. P.; Manne, S.; Bocek, D.; Hansma, P. K. *Rev. Sci. Instrum.* **1993**, *64* (2), 75.

(24) Fernández Estarlich, F.; Lewey, S. A.; Nevell, T. G.; Thorpe, A. A.; Tsibouklis, J.: Upton, A. C. *Biofouling* **2000**, *16* (2−4), 263.

(25) Wagner, C. D.; Davis, L. E.; Zeller, M. V.; Taylor, J. A.; Raymond, R. H.; Gale, L. H. *Surf. Interface Anal.* **1981**, *3*, 211.

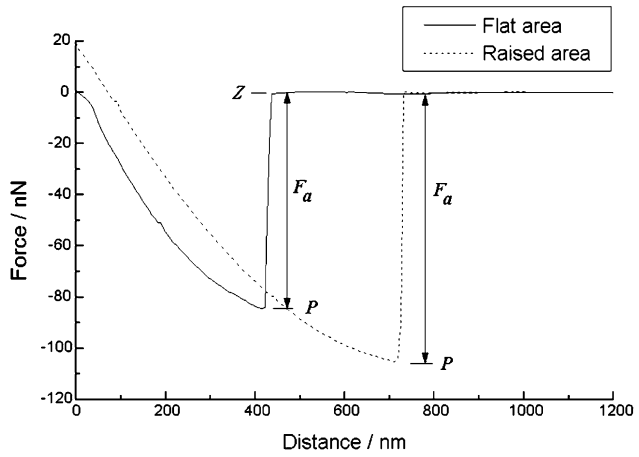

Figure 5. Adhesion of a silicon nitride tip to the surface of GE-RTV11 (deflection of the flexible cantilever (K = 0.24 N m^{-1}) against displacement of the tip from the surface; P = pull-off point; Z = zero-force line; adhesion (pull-off) force F_a = [P − Z]: (a) flat surface (···); (b) raised surface feature (—)).

as the tip is pushed into the sample [right to left]) shows a much steeper gradient than that for the flat surface. Comparison of these curves with that for the surface of stainless steel (hard, control) shows that appreciable indentation into both surface regions had occurred, although the surface of the protrusion was considerably stiffer than that of the flat elastomer.

To visualize variations in stiffness across the film surface, the nanoindentation measured at a constant applied force (178 nN, chosen to maximize the contrast) has been plotted as a gray scale map, together with the corresponding topographic image of the same selected typical area, Figure 4. In this indentation (surface stiffness) map, lighter shades correspond to greater indentation and hence to softer material. The high features seen in the topography correspond to relatively stiff (dark) areas of the polymer, while the flat areas are softer, showing greater indentation in the stiffness map. These observations are consistent with the protrusions consisting of, relatively hard, calcium carbonate filler particles. The higher stiffness in these regions probably reflects the force required to push a particle into the bulk elastomer, rather than the stiffness of the particle itself. Interestingly, the indentation map reveals soft (bright) regions surrounding the hard particles (boundary thickness = 170 nm; std dev = 60 nm). The indentation measurements (Figure 3, region d: shown by distinct changes in gradient) appear to give some indication of the polymer film thickness being consistent with the apparent boundary layer seen in Figure 4b. There are also some of the softer areas dispersed over flat regions: they may consist of material of lower packing density (due to differences in degree of cross-linking); alternatively, this may be due to the presence of a substantial number of very small particles of filler in these regions (indentation images of unfilled samples did not exhibit this feature).

Adhesion Mapping with Topography. To investigate further the surfaces of the protrusions on RTV11, adhesion force mapping measurements were made, Figure 5. For each determination, the adhesion force (F_a) was obtained as the difference between the zero-force line (Z) and the pull-off point (P). Forces measured over the feature were less than those for the flat areas of the surface. In a gray scale map of values of F_a for a typical area, together with the corresponding topography, Figure 6, brighter areas represent higher topography [left] and higher adhesion values [right]. This figure illustrates the consistent finding that adhesion forces are lower in the regions corresponding to the protrusions; as the AFM tip was moved away from a particle, F_a increased progressively to a maximum value of ca. 100 nN. Similar experiments on the surface of the elastomer from which filler had been removed gave homogeneous (featureless) adhesion maps; also with typical adhesion values of ca. 100 nN. Hence the film covering protruding particles was less adhesive than the bulk elastomer. The possibility should also be considered, that the greater stiffness of the particles could have caused a change in adhesion force in these areas. This however is less likely, because the approach curves, which were obtained under the conditions used for adhesion mapping, showed no hysteresis, such as might have been expected for the indentation of a polymeric material.[26] With the flexible cantilever used for adhesion measurements, no significant indentation occurred, even of the softer thin film covering each protruding particle of filler.

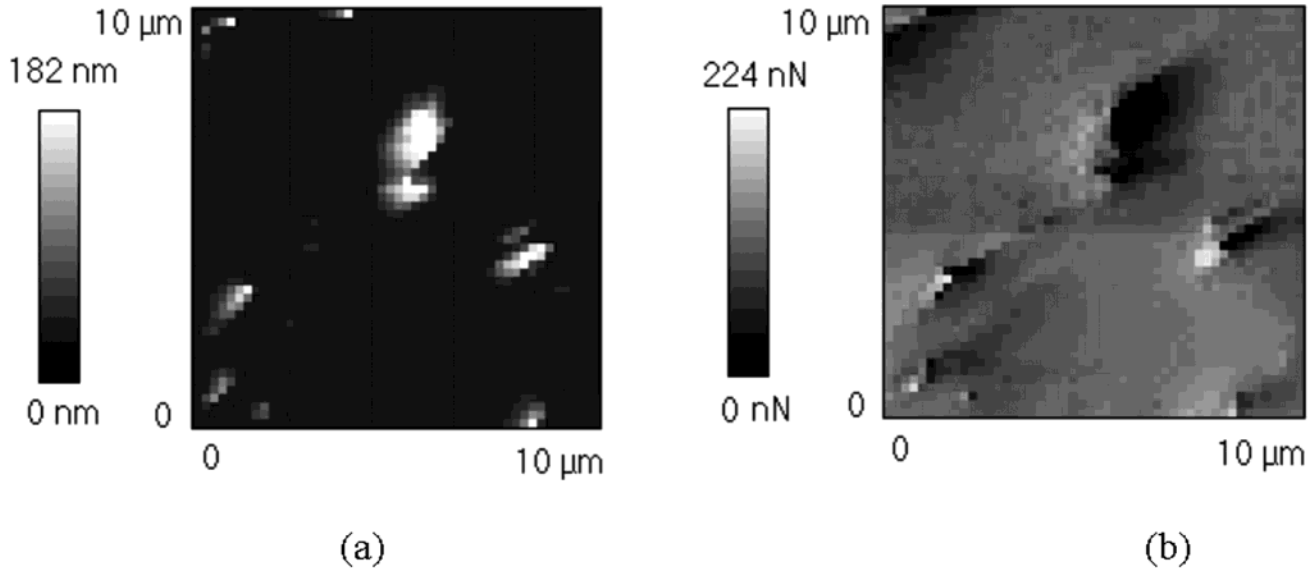

Figure 6. Adhesion mapping of a selected area of the surface of GE-RTV11, using a flexible cantilever (K = 0.24 N m^{-1}) with a silicon nitride tip: (a) topographic image; (b) adhesion image.

Discussion

The combination of the topographic imaging with point-by-point adhesion and indentation mapping has shown greater detail of the surface than topographic imaging alone and has clarified the nature of the surface features of the filled silicone elastomer. The surfaces of these features were stiffer than those of areas between them, but were still indented measurably by the tip of the stiff cantilever. Individual indentation measurements made over protruding features probably caused the underlying particles to be forced into the bulk elastomer. The adhesion measurements, which were sensitive only to the surface material, have established that the thin film covering each protruding particle differed from the surrounding polymer. This also corresponded with the "soft" surface boundary regions around each particle that were observed in the indentation measurements. Similar measurements for blended polymer structures support these findings and illustrate the general utility of these AFM methods.[27]

Conclusions

Three experimental techniques in AFM, viz., topographic imaging, adhesion force mapping, and indentation mapping, have been used to investigate the surface of an elastomeric filled silicone coating. Topographic observations have shown randomly distributed protruding features, of a similar size range as filler particles. Comparison of indentation and adhesion maps with topographic images has established that the particles of filler were each covered by a thin layer of softer and less adhesive material, thereby further demonstrating the value of combining the three distinct and complementary AFM techniques of surface analysis. Since the resolutions of the adhesion and indentation maps are limited only by the geometry of the AFM tip, it may be possible to differentiate with these techniques features as small as 10 nm.

LA0110747

(26) Burnham, N. A.; Colton, R. J. *J. Vac. Sci. Technol. A* **1989**, *7* (*4*), 2906.

(27) Eaton, P. J.; Smith, J. R.; Graham, P.; Smart, J. D.; Nevell, T. G.; Tsibouklis, J. *Langmuir* **2002**, *18*, 3387.